# $(t,p)$ studies of $^{52}$Ti, $^{53}$V, and $^{57}$Mn and tests of mixed-configuration shell-model calculations

J. F. Mateja* and L. R. Medsker†
*Department of Physics, Florida State University, Tallahassee, Florida 32306*

C. P. Browne and J. D. Zumbro
*Department of Physics, University of Notre Dame, Notre Dame, Indiana 46556*

H. T. Fortune and R. Middleton
*Department of Physics, University of Pennsylvania, Philadelphia, Pennsylvania 19104*

J. B. McGrory
*Oak Ridge National Laboratory, Oak Ridge, Tennessee 37830*

(Received 21 January 1980)

Nineteen levels up to 5.1 MeV in $^{52}$Ti and 52 levels up to 4.7 MeV in $^{53}$V have been identified using the $^{50}$Ti$(t,p)$ and $^{51}$V$(t,p)$ reactions. Measured angular distributions were compared with results of distorted-wave Born-approximation calculations. In $^{52}$Ti, the experimental angular distributions agree with distorted-wave Born-approximation shapes for four states whose $J^\pi$ values were previously known. For six levels we make clear $L$ (and hence $J^\pi$) assignments, and we present tentative assignments for six additional levels. In $^{53}$V, no discrepancies were found between spin assignments suggested in earlier studies and the spin limitations imposed by the $L$ values extracted from the $(t,p)$ angular distributions. The present results along with the experimental results from an earlier $^{55}$Mn$(t,p)^{57}$Mn study were used to test mixed-configuration shell-model calculations for the three residual nuclei. The agreement between the experimental and predicted level schemes is good up to 1.5 MeV, but above this energy a number of levels are present which are not predicted by the calculation. The shell-model wave functions were also used to calculate spectroscopic amplitudes for two-nucleon transfer reactions. In all three residual nuclei, fair agreement is found between the experimental strengths and the strengths predicted by the calculations.

[NUCLEAR REACTIONS $^{50}$Ti$(t,p)^{52}$Ti and $^{51}$V$(t,p)^{53}$V, $E_t$=15 MeV, $\sigma(\theta, E_p)$, DWBA analysis; $^{52}$Ti and $^{53}$V deduced $L, J, \pi$, enhancement factors; shell-model calculations; $^{57}$Mn, DWBA analysis, deduced enhancement factors.]

## I. INTRODUCTION

Several shell-model calculations have now been performed in the region of the $1f_{7/2}$ subshell.[1-7] The present work was undertaken to test the results of one of these shell-model calculations[1] for nuclei with $z$ of 22, 23, and 25 and $N=30$. In this calculation an inert $^{48}$Ca core was assumed with the valence protons restricted to the $1f_{7/2}$ subshell and the valence neutrons occupying the $2p_{3/2}$, $1f_{5/2}$, and $2p_{1/2}$ subshells. A Hamiltonian was used which led to a good fit to selected data in this mass region. The agreement between the predicted and experimental level schemes for excitation energies below 2 MeV was satisfactory. However, when an effective Hamiltonian is used, agreement between calculated and experimental level schemes does not mean that an accurate description of the nucleus has been obtained. Correct level schemes can be obtained with incorrect wave functions. One additional test of shell-model wave functions is the calculation of cross sections for nucleon-transfer reactions, for which the $(t,p)$ reaction is of particular usefulness. A comparison of experimental cross sections with theoretical cross sections calculated with spectroscopic amplitudes predicted by shell-model wave functions tests not only the magnitudes of the various wave-function components but also their phases. Such a comparison has been reported for the $^{54}$Fe$(t,p)^{56}$Fe reaction[1] and the calculated cross sections accurately reproduced the relative experimental cross sections for the low-lying $^{56}$Fe levels. In a subsequent study of the $^{55}$Mn$(t,p)^{57}$Mn reaction,[8] the shell-model two-nucleon-transfer spectroscopic amplitudes, when used in a distorted-wave Born-approximation (DWBA) analysis, led to agreement between the shapes of the calculated and experimental angular distributions and reasonable agreement in magnitudes. (In the shell-model calculation for $^{57}$Mn, the four neutrons were also restricted to the $2p_{3/2}$, $1f_{5/2}$, and $2p_{1/2}$ subshells.)

We present here our results for the $^{50}$Ti$(t,p)^{52}$Ti and $^{51}$V$(t,p)^{53}$V reactions in comparison with the earlier $^{55}$Mn$(t,p)^{57}$Mn results. The experimental $^{57}$Mn angular distributions have been reanalyzed

 

using a set of triton parameters consistent with those used in the analysis of the present reactions.

## II. EXPERIMENTAL PROCEDURE

The $^{50}$Ti$(t,p)^{52}$Ti and $^{51}$V$(t,p)^{53}$V experiments were performed with a 15-MeV triton beam made possible by the temporary installation of a tritium sputter ion source on the University of Pennsylvania FN tandem Van de Graaff accelerator. The $^{50}$Ti and $^{51}$V targets, each approximately 80 $\mu$g/cm$^2$ thick and evaporated onto carbon backings, were enriched to 76% and 99%, respectively. The principal contaminant in the $^{50}$Ti target was an 18% $^{48}$Ti impurity. The reaction protons were momentum analyzed with a multi-angle spectrograph over a laboratory angular range from 3.75° to 86.25° in 7.5° intervals. Absorber foils were placed directly over the nuclear emulsion plates used to detect the protons in order to eliminate all other reaction particles. An energy calibration for the focal plane surfaces was obtained using the $^{12}$C$(t,p)^{14}$C and $^{16}$O$(t,p)^{18}$O contaminant peaks along with previously reported ground state $Q$ values for both the $^{52}$Ti and $^{53}$V experiments.[9] For the $^{53}$V study, excitation energies for $^{53}$V levels from the $\beta$-decay study of Parks *et al.*[10] were also used in the calibration. The estimated energy uncertainty for levels below 2 MeV in both studies is 4 keV whereas above 2 MeV the uncertainty is ~8 keV. The experimental resolution was about 25 keV full width at half maximum (FWHM) in both experiments.

The earlier $^{55}$Mn$(t,p)^{57}$Mn experiment[8] was performed with a 17-MeV triton beam from the Los Alamos tandem Van de Graaff accelerator. The $^{55}$Mn target thickness was approximately 80 $\mu$g/cm$^2$ on a 20 $\mu$g/cm$^2$ carbon backing. The reaction protons were recorded with the Los Alamos Q3D type II spectrograph.

For both the Pennsylvania and Los Alamos experiments, elastically scattered tritons were recorded with silicon surface-barrier detectors positioned in the scattering chamber at 40° for the $^{52}$Ti and $^{53}$V experiments and at 30° for the $^{57}$Mn work. These elastically scattered tritons were used to establish an absolute cross section by normalizing to optical-model calculations using the parameters listed in Table I. The uncertainty in the absolute cross section using this technique is estimated to be ~35%. The monitor was also used to obtain accurate relative cross sections from angle to angle for the $^{57}$Mn experiment whereas no such normalization was required for the $^{52}$Ti and $^{53}$V studies as all angles were recorded simultaneously.

TABLE I. Optical-model parameters used in the distorted-wave analysis.

| Particle | $V$ (MeV) | $W$ (MeV) | $W_d$ (MeV) | $r_0$ (fm) | $a_0$ (fm) | $r_I$ (fm) | $a_I$ (fm) |
|---|---|---|---|---|---|---|---|
| $t$ | 165.4 | 16.4 | 0.0 | 1.16 | 0.75 | 1.50 | 0.75 |
| $p$ | a | 0.0 | a | 1.25 | 0.65 | 1.25 | 0.47 |
| $n$ | b | | | 1.27 | 0.67 | | |

[a] The proton real and imaginary well depths, respectively, were as follows: for $^{52}$Ti, 52.87 and 11.19 MeV; for $^{53}$V, 52.87 and 11.27 MeV; for $^{57}$Mn, 46.70 and 11.55 MeV.

[b] Adjusted to give a binding energy to each particle of $0.5[Q(t,p)+8.482]$ MeV.

## III. RESULTS

Displayed in Figs. 1 and 2 are proton spectra for the $^{50}$Ti$(t,p)^{52}$Ti and $^{51}$V$(t,p)^{53}$V reactions. The contaminant groups from $^{12}$C, $^{14}$N, and $^{16}$O are labeled in Fig. 1. Figure 1 also shows peaks arising from the $^{48}$Ti impurity in the target material. Four $^{16}$N levels with energies 0, 120, 296, and 396 keV were identified as were levels in $^{50}$Ti which correspond in energy to those seen most strongly in an earlier $^{48}$Ti$(t,p)^{50}$Ti study by Hinds and Middleton.[11] All other $^{50}$Ti levels in the Hinds and Middleton work had cross sections which were lower by a factor of ~8. These weak levels were not seen in the present study.

The $^{52}$Ti and $^{53}$V levels observed in this experiment along with a tabulation of levels previously reported for these nuclei are listed in Tables II and III, respectively. Nineteen levels up to 5.1 MeV in $^{52}$Ti and 53 levels up to 4.7 MeV in $^{53}$V have been observed. Of these, 10 levels in $^{52}$Ti and 13 levels in $^{53}$V were previously unreported. An-

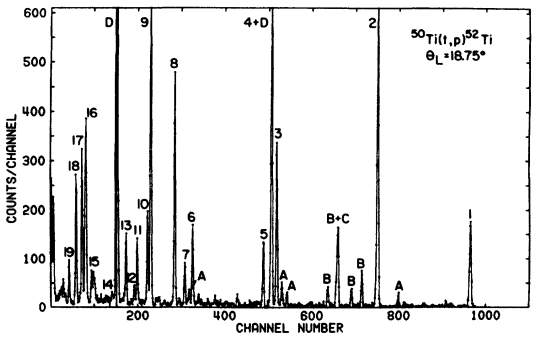


FIG. 1. Proton spectrum for the $^{50}$Ti$(t,p)^{52}$Ti reaction. Peaks labeled *A* are $^{50}$Ti contaminants with excitation energies of 5697, 7041, 7094, and 8292 keV; those labeled *B* are $^{16}$N levels with energies of 0, 120, 296, and 396 keV; the peak labeled *C* is the $^{14}$C ground state; and those labeled *D* are $^{18}$O levels at energies of 0 and 1982 keV. The bombarding energy was 15 MeV.

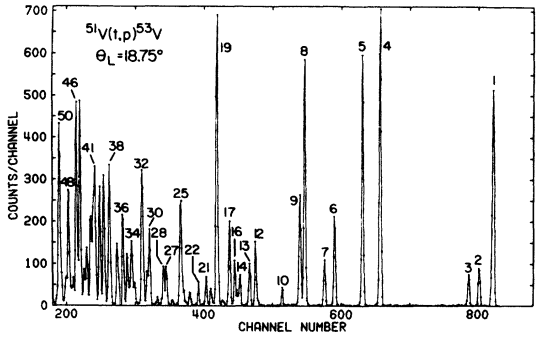


FIG. 2. Proton spectrum for the $^{51}$V($t$, $p$)$^{53}$V reaction. The bombarding energy was 15 MeV.

gular distributions have been extracted for all levels up to 4.8 MeV in $^{52}$Ti and for states up to 3.0 MeV in $^{53}$V (see Figs. 3 through 6).

The spins and parities of levels in $^{52}$Ti were determined from a comparison between the experimental angular distributions and those calculated using the distorted-wave Born approximation (see section on DWBA analysis for details). Although $^{52}$Ti has been studied previously via the $^{50}$Ti($t$, $p\gamma$) reaction[12] and spin assignments made from particle-gamma correlations, many of the less strongly populated levels were unobserved in the earlier work. For those levels observed

TABLE II. Comparison of excitation energies and spins for states in $^{52}$Ti measured in the present $^{50}$Ti($t$, $p$)$^{52}$Ti experiment with previously reported results.

| Peak No. | Present experiment $E_x$ (keV) | $J^\pi$ | $^{50}$Ti($t$,$p$)$^{52}$Ti[a] $E_x$ (keV) | $J^\pi$ |
|---|---|---|---|---|
| 1 | 0.0 | $0^+$ | 0.0 | $0^+$ |
| 2 | 1050 | $2^+$ | 1047.1 | $2^+$ |
| 3 | 2262 | $2^+$ | 2259.4 | 2 |
| 4 | 2316 | $4^+$ | 2317[b] | $(4^+)$ |
| 5 | 2429 | $2^+$ | 2427.5 | $2^+$ |
| | | | 3027[b] | $(6^+)$ |
| | | | 3200[b] | |
| 6 | 3346 | $4^+$ | | |
| 7 | 3447 | $3^-$ | | |
| 8 | 3583 | $2^+$ | 3582.5 | |
| 9 | 3872 | $3^-$ | | |
| 10 | 3916 | $2^+$ | 3900 | 1,2,3 |
| 11 | 4058 | $(4^+)$ | | |
| 12 | 4098 | $0^+,1^-$ | | |
| 13 | 4212 | $0^+,1^-$ | 4230 | 1 |
| 14 | 4324 | $1^-,0^+$ | 4300 | |
| 15 | 4691 | $1^-,0^+$ | | |
| 16 | 4772 | $(2^+)$ | | |
| 17 | 4823 | | | |
| 18 | 4909 | | | |
| 19 | 5010 | | | |

[a] Reference 12.
[b] Reference 13.

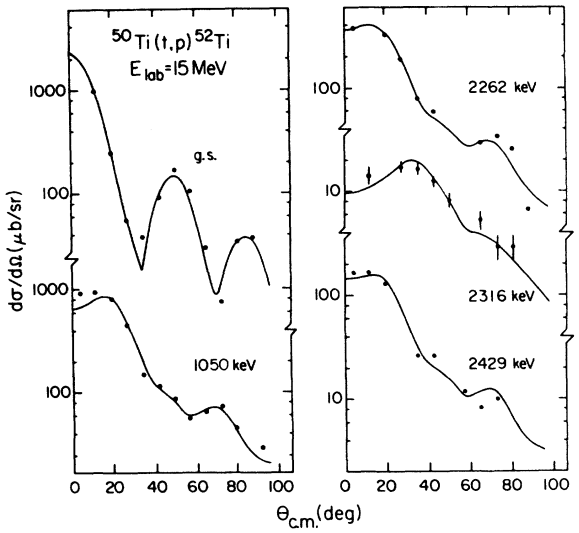


FIG. 3. Angular distributions for states in $^{52}$Ti. The curves are from DWBA calculations which employed shell model two-nucleon transfer spectroscopic amplitudes.

in both experiments, there are no disagreements in the spin assignments. In addition to these levels, spin and parity assignments are made to nine $^{52}$Ti levels which are reported here for the first time.

For odd-mass targets, a unique spin assignment for a level in the residual nucleus can be made only when the angular distribution for the level shows clear evidence of an $L = 0$ admixture. In such a case the final spin would be restricted to $J^\pi = \frac{7}{2}^-$ in $^{53}$V since the target ground-state spin is $\frac{7}{2}^-$. The ground state, 1852-, and 2524-keV levels in $^{53}$V all exhibited clear $L = 0$ components in their

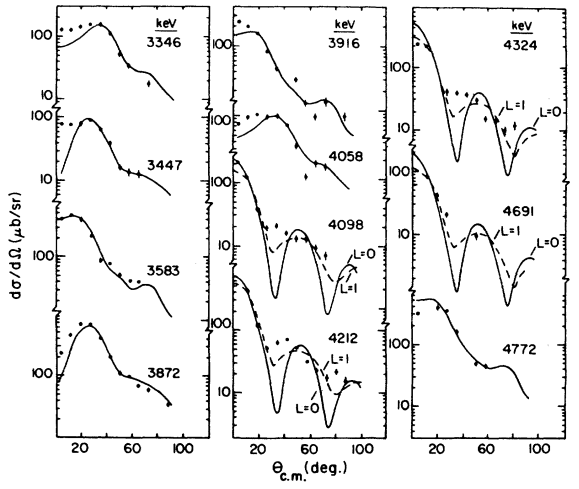


FIG. 4. Angular distributions for levels in $^{52}$Ti. The curves were generated in a DWBA analysis which used single two-nucleon configurations.

TABLE III. Comparison of excitation energies and spins for levels in $^{53}$V measured in the present $^{51}$V$(t,p)^{53}$V experiment with previously reported results.

| Peak No. | Present experiment $E_x$ (keV) | $L$ | $J^\pi$ | $^{51}$V$(t,p)^{53}$V[a] $E_x$ (keV) | $J^\pi$ | $^{51}$V$(t,p\gamma)^{53}$V[b] $^{53}$Ti$(\beta)^{53}$V[c] $E_x$ (keV) | $J^\pi$ |
|---|---|---|---|---|---|---|---|
| 1 | 0.0 | 0+2+4 | $\frac{7}{2}^-$ | 0.0 | $\frac{7}{2}$ | 0.0 | $\frac{7}{2}^-$ |
| 2 | 127 | 2+4 | $(\frac{5}{2}^-)$ | 129 | | 127.6 | $(\frac{5}{2}^-)$ |
| 3 | 226 | 2+4 | $(\frac{3}{2}^-)$ | 230 | | 228.4 | $(\frac{3}{2}^-)$ |
| 4 | 1093 | 2+4 | $(\frac{11}{2}^-)$ | 1095 | | 1090 | $(\frac{11}{2}^-)$ |
| 5 | 1269 | 2+4 | $(\frac{9}{2}^-)$ | 1269 | | 1265 | $(\frac{9}{2}^-)$ |
| 6 | 1551 | 2+4 | $(\frac{5}{2}^-)$ | 1555 | | 1549.3 | $\frac{3}{2}^-, \frac{5}{2}^-$ |
| 7 | 1652 | 2+4 | $(\frac{9}{2}^-)$ | 1656 | | 1652 | |
| 8 | 1852 | 0+2+4 | $\frac{7}{2}^-$ | 1864 | $(\frac{7}{2}^-)$ | 1856 | |
| 9 | 1901 | 2+4 | $(\frac{3}{2}^-)$ | 1903 | | 1903.8 | $\frac{3}{2}^-, \frac{5}{2}^-$ |
| 10 | 2079 | 2+4 | $(\frac{3}{2}^-)$ | 2085 | | 2084.1 | $\frac{3}{2}^-, \frac{5}{2}^-$ |
| 11 | 2332 | | | | | | |
| 12 | 2357 | | | 2363 | | | |
| 13 | 2421 | | | 2428 | $(\frac{7}{2}^-)$ | | |
| 14 | 2524 | | | 2531 | $\frac{7}{2}^-$ | | |
| 15 | 2550 | | | | | 2550 | $\frac{1}{2}^-, \frac{3}{2}^-, \frac{5}{2}^-$ |
| 16 | 2576 | | | 2578 | | 2584.1 | $\frac{3}{2}^-, \frac{5}{2}^-$ |
| 17 | 2636 | | | 2639 | | | |
| 18 | 2706 | | | 2701 | | | |
| 19 | 2772 | | | 2774 | | 2774 | |
| 20 | 2831 | | | 2831 | | 2829.5 | $\frac{3}{2}^-, \frac{5}{2}^-$ |
| 21 | 2888 | | | 2885 | | | |
| 22 | 2967 | | | 2931<br>2966 | | 2931 | $\frac{1}{2}^-, \frac{3}{2}^-, \frac{5}{2}^-$ |
| 23 | 3062 | | | 3066 | | | |
| 24 | 3107 | | | 3094 | | | |
| 25 | 3158 | | | 3156 | | | |
| 26 | 3263 | | | | | | |
| 27 | 3320 | | | 3320 | | | |
| 28 | 3348 | | | 3342 | | | |
| 29 | 3411 | | | 3412 | | | |
| 30 | 3492 | | | 3487 | | | |
| 31 | 3520 | | | 3515 | | | |
| 32 | 3573 | | | 3571 | | | |
| 33 | 3661 | | | 3658 | | | |
| 34 | 3692 | | | 3688 | | | |
| 35 | 3738 | | | 3738 | | | |
| 36 | 3784 | | | 3788 | | | |

TABLE II. (*Continued*)

| Peak No. | $E_x$ (keV) | $L$ | $J^\pi$ | $E_x$ (keV) | $J^\pi$ | $^{51}$V$(t,p\gamma)^{53}$V[b] $^{53}$Ti$(\beta)^{53}$V[c] $E_x$ (keV) | $J^\pi$ |
|---|---|---|---|---|---|---|---|
| 37 | 3841 | | | 3840 | | | |
| 38 | 3947 | | | 3950 | | | |
| 39 | 3999 | | | 4000 | | | |
| 40 | 4042 | | | 4050 | | | |
| 41 | 4097 | | | 4100 | | | |
| 42 | 4143 | | | | | | |
| 43 | 4187 | | | | | | |
| 44 | 4218 | | | | | | |
| 45 | 4263 | | | | | | |
| 46 | 4306 | | | | | | |
| 47 | 4345 | | | | | | |
| 48 | 4392 | | | | | | |
| 49 | 4428 | | | | | | |
| 50 | 4497 | | | | | | |
| 51 | 4593 | | | | | | |
| 52 | 4669 | | | | | | |

[a] Reference 14.
[b] Reference 15.
[c] Reference 10.

angular distributions, implying that these states have $J^\pi = \frac{7}{2}^-$. A weak $L = 0$ component may also be present in the angular distribution for a level at 2421 keV. An angular momentum transfer of $L = 2$, when coupled to the $J = \frac{7}{2}$ ground state spin of $^{51}$V, restricts the spin and parity of levels in $^{53}$V from $J^\pi = \frac{3}{2}^-$ to $\frac{11}{2}^-$, while an $L = 4$ angular momentum transfer allows spins and parities from $J^\pi = \frac{1}{2}^-$ to $\frac{15}{2}^-$. In general, varying admixtures of $L = 2$ and 4 will occur for any level with $J^\pi = \frac{3}{2}^-$ to $\frac{11}{2}^-$. Depending on the $L = 2$ and 4 admixtures, the shape of the angular distribution will be strongly affected. Because of this ambiguity, only those experimental levels which could be associated with a shell-model state on the basis of energy and a previously determined spin were analyzed. From the shell-model wave functions for these states, two-nucleon-transfer spectroscopic amplitudes were calculated. An important test of these shell-model wave functions is whether or not they lead to the correct transferred angular momentum admixture. The assumed $J^\pi$ of the $^{53}$V levels, along with the angular momentum transfer predicted by the shell-model calculations, are listed in Table III.

The experimental results presented here for the $^{55}$Mn$(t,p)^{57}$Mn reaction were taken from Ref. 8 with the exception of the spin for the 1375-keV $^{57}$Mn level. It was subsequently shown in the $\beta$-decay study of Davids *et al.*[16] that the spin of this level is either $\frac{3}{2}$ or $\frac{5}{2}$ as this level is fed by the $\beta$ decay of $^{57}$Cr. (The spin of $\frac{9}{2}$ suggested in Ref. 8 was based solely on a comparison in energy of this state and a state predicted by the shell-model calculation.) The 1477-keV level was the only level not fed by $\beta$ decay in this excitation region in $^{57}$Mn; therefore, it is the only level which can have a spin $\gtrsim \frac{7}{2}^-$ according to the standard Gamow-Teller rules for allowed $\beta$ decay.

## IV. DWBA ANALYSIS

Microscopic distorted-wave Born approximation calculations have been made using the computer code DWUCK.[17] For levels in $^{53}$V and $^{57}$Mn below approximately 2 MeV and in $^{52}$Ti below 2.5 MeV, two-nucleon spectroscopic amplitudes, generated from the shell-model wave functions discussed previously, were used in the DWBA calculations. Above these excitation energies,

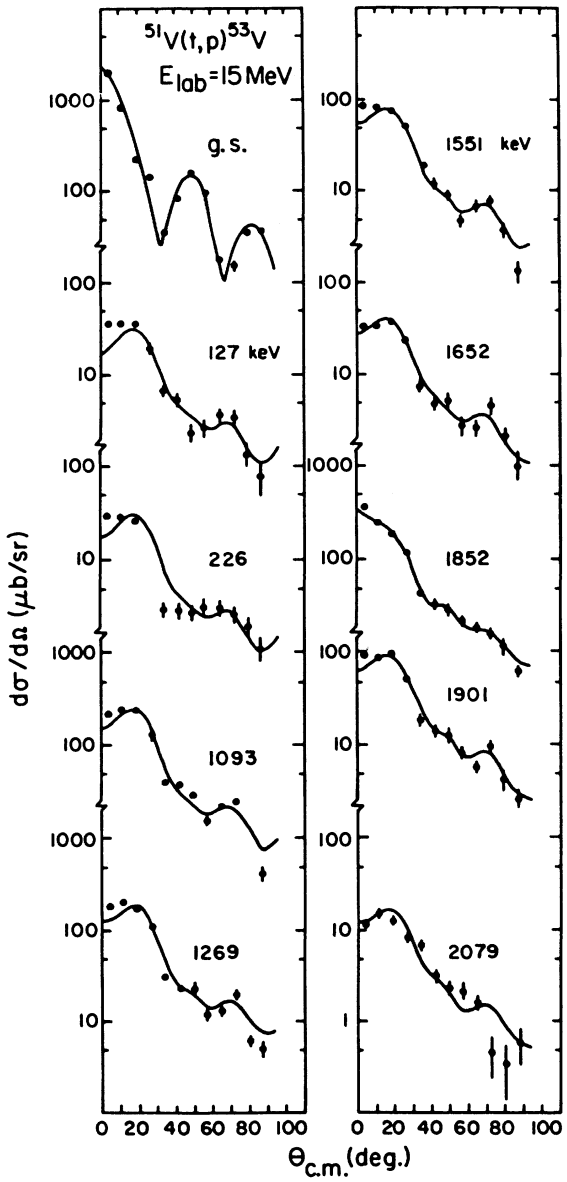


FIG. 5. Angular distributions for states in $^{53}$V. The curves are from DWBA calculations which used shell model two-nucleon transfer spectroscopic amplitudes.

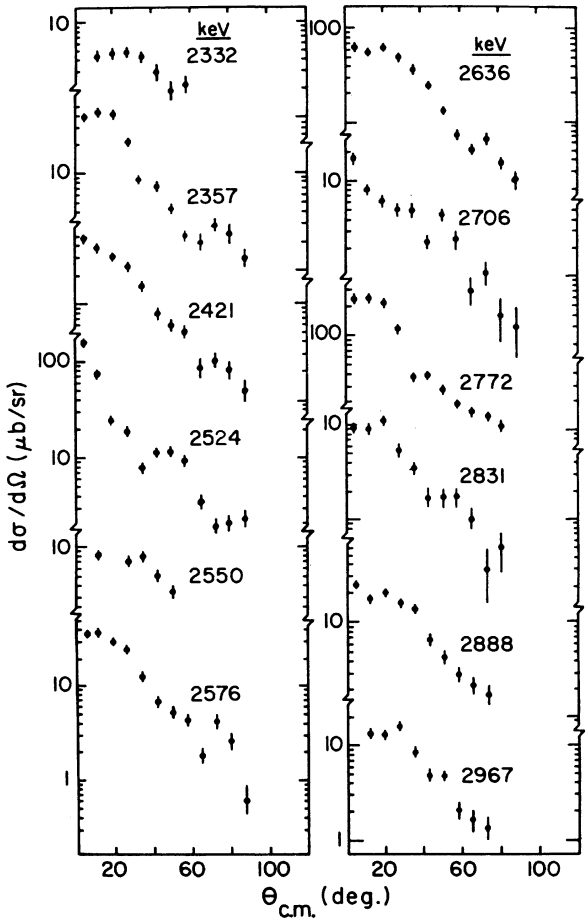


FIG. 6. Angular distributions for states in $^{53}$V.

the correspondence between shell-model and experimental levels was unclear. However, for the $^{52}$Ti levels above 2.5 MeV, DWBA calculations have been made using pure two-nucleon configurations.

The triton parameters used in these calculations were taken from an earlier $(t,p)$ study on Ti by Casten *et al.*[18] The proton parameters were obtained from the global proton parameter set of Perry.[19] The proton real and imaginary well depths had to be adjusted slightly in all three cases to obtain good phase agreement between the experimental and calculated angular distributions. The optical-model and bound-state parameters used in the analyses are listed in Table I.

The DWBA calculations were normalized as follows:

$$d\sigma/d\Omega_{\text{exp}} = N\epsilon \frac{2J_B+1}{2J_A+1} (T_A N_A 11 | T_B N_B)^2 \times \sum_L (2L+1)^{-1} \sigma^L_{\text{DWUCK}}(\theta) . \quad (1)$$

The quantities $J_A$, $T_A$, $N_A$ and $J_B$, $T_B$, $N_B$ are the spin, isospin, and isospin projection for the target ground state and levels in the residual nucleus, respectively. The Clebsch-Gordan coefficient accounts for the change in isospin due to the transferred neutron pair. In the present cases, this factor is one. The total transferred angular momentum $J$ is equal to the transferred orbital angular momentum $L$ according to the selection rules for a direct, single-step $(t,p)$ reaction. A value for $N$ of $218 \pm 33$ was obtained by Flynn *et al.*[20] when a standard set of optical-model and bound-state parameters like those used in the

present analysis were used in the DWBA code DWUCK. The remaining quantity, the enhancement factor $\epsilon$, is then a measure of how well the experimental data are described by the calculation. An exact prediction would produce an $\epsilon$ equal to one.

The spectroscopic amplitudes for all allowed two-nucleon configurations for each level were calculated using the shell-model wave functions. These spectroscopic amplitudes are listed in Tables IV and V. Columns one and two identify the shell-model level by energy and spin, respectively. The third column lists the allowed $L$ transfers to each level while the last six columns list the values of the two-nucleon spectroscopic amplitudes. The experimental level scheme and its corresponding shell-model spectrum are shown in Fig. 7 for the three nuclei studied. The dashed lines in Fig. 7 indicate which shell-model level has been associated with each experimental level. This correspondence between experimental and shell-model levels has been made based on both the energy and spin of the level. Only those experimental states which have spin assignments, or at least spin limitations, have been included in this analysis. No levels above 2 MeV in $^{53}$V and $^{57}$Mn or levels above 2.5 MeV in $^{52}$Ti have been included in this analysis as the correspondence between the experimental and shell-model spectra is unclear.

For the levels in $^{52}$Ti above 2.5 MeV, angular distributions were generated using pure two-nucleon configurations. Since only a single $L$ transfer exists to a given level for $(t,p)$ reactions on even-mass target nuclei, the shape of the angular distribution is unambiguously determined.

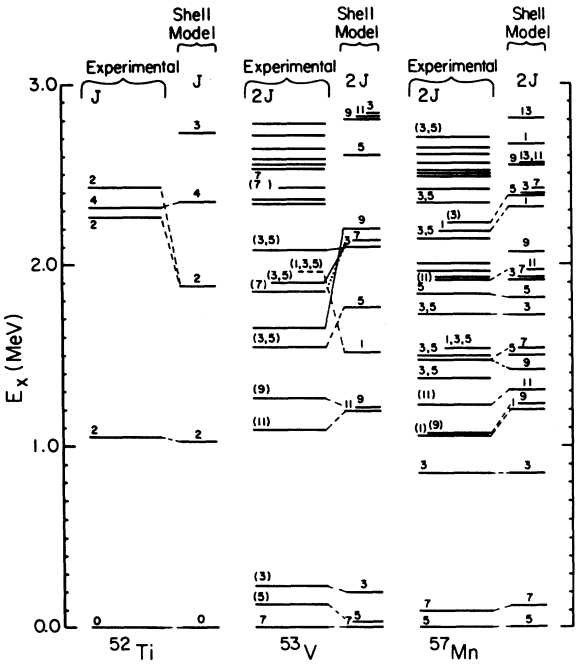


FIG. 7. Experimental and theoretical level schemes for the $^{52}$Ti, $^{53}$V, and $^{57}$Mn nuclei. The dashed lines indicate the correspondence between experimental and theoretical levels used in this study.

TABLE IV. Two-nucleon transfer spectroscopic amplitudes calculated using shell-model wave functions for the $^{50}$Ti$(t,p)^{52}$Ti reaction. The first two columns give the excitation energy and spin of the shell-model predicted states in $^{52}$Ti.

| $E_x$ | $J$ | $L$ | $(p_{3/2})^2$ | $(f_{5/2})^2$ | $(p_{1/2})^2$ | $(p_{3/2},f_{5/2})$ | $(p_{3/2},p_{1/2})$ | $(f_{5/2},p_{1/2})$ |
|---|---|---|---|---|---|---|---|---|
| 0 | 0 | 0 | −0.845 | −0.188 | −0.251 | | | |
| 1028 | 2 | 2 | −0.568 | −0.067 | | 0.087 | −0.437 | 0.108 |
| 1879 | 2 | 2 | 0.286 | 0.009 | | 0.011 | 0.272 | −0.021 |
| 2346 | 4 | 4 | | −0.045 | | 0.259 | | |
| 2725 | 3 | 3 | | | | −0.052 | | 0.027 |
| 3270 | 2 | 2 | −0.650 | 0.022 | | −0.040 | 0.271 | −0.059 |
| 3565 | 1 | 1 | | | | 0.028 | 0.554 | |
| 3679 | 4 | 4 | | −0.098 | | 0.617 | | |
| 4036 | 4 | 4 | | 0.047 | | −0.179 | | |
| 4219 | 0 | 0 | −0.225 | 0.260 | 0.564 | | | |
| 4304 | 4 | 4 | | −0.034 | | 0.198 | | |
| 4360 | 2 | 2 | 0.049 | 0.108 | | −0.383 | −0.542 | −0.246 |
| 4556 | 1 | 1 | | | | −0.030 | 0.591 | |
| 4597 | 3 | 3 | | | | 0.425 | | −0.014 |
| 4758 | 1 | 1 | | | | 0.708 | 0.041 | |
| 4978 | 0 | 0 | −0.442 | 0.354 | 0.078 | | | |
| 5221 | 3 | 3 | | | | 0.567 | | 0.080 |
| 5237 | 0 | 0 | 0.167 | 0.528 | −0.286 | | | |
| 5609 | 3 | 3 | | | | 0.098 | | 0.312 |
| 6197 | 1 | 1 | | | | | −0.509 | |

TABLE V. Two-nucleon transfer spectroscopic amplitudes calculated using shell model wave functions for the $^{51}V(t,p)^{53}V$ reaction. The first two columns list the excitation energy and spin of the shell model predicted $^{53}V$ states.

| $E_x$ | $J$ | $L$ | $(p_{3/2})^2$ | $(f_{5/2})^2$ | $(p_{1/2})^2$ | $(p_{3/2},f_{5/2})$ | $(p_{3/2},p_{1/2})$ | $(f_{5/2},p_{1/2})$ |
|---|---|---|---|---|---|---|---|---|
| 0 | $\frac{7}{2}$ | 0 | 0.753 | 0.194 | 0.250 | | | |
| | | 2 | 0.159 | 0.029 | | −0.035 | 0.154 | −0.041 |
| | | 4 | 0.004 | | | −0.009 | | |
| 26 | $\frac{5}{2}$ | 2 | 0.341 | 0.080 | | −0.094 | 0.229 | −0.097 |
| | | 4 | | 0.040 | | −0.160 | | |
| 192 | $\frac{3}{2}$ | 2 | −0.355 | −0.054 | | 0.063 | −0.366 | 0.137 |
| | | 4 | | 0.048 | | −0.189 | | |
| 1196 | $\frac{11}{2}$ | 2 | −0.551 | −0.075 | | 0.095 | −0.046 | 0.132 |
| | | 4 | | −0.006 | | 0.038 | | |
| 1213 | $\frac{9}{2}$ | 2 | 0.443 | 0.053 | | −0.062 | 0.402 | −0.103 |
| | | 4 | | 0.033 | | −0.171 | | |
| 1516 | $\frac{1}{2}$ | 4 | | −0.022 | | 0.137 | | |
| 1763 | $\frac{5}{2}$ | 2 | 0.430 | 0.020 | | 0.028 | 0.446 | −0.020 |
| | | 4 | | −0.002 | | 0.070 | | |
| 2097 | $\frac{3}{2}$ | 2 | −0.573 | −0.022 | | 0.051 | −0.322 | 0.017 |
| | | 4 | | −0.079 | | 0.397 | | |
| 2131 | $\frac{7}{2}$ | 0 | 0.329 | 0.080 | 0.023 | | | |
| | | 2 | −0.650 | −0.081 | | 0.108 | −0.456 | 0.130 |
| | | 4 | | 0.007 | | −0.017 | | |
| 2197 | $\frac{9}{2}$ | 2 | 0.516 | 0.060 | | −0.082 | 0.171 | −0.031 |
| | | 4 | | −0.042 | | 0.185 | | |
| 2600 | $\frac{5}{2}$ | 2 | 0.224 | −0.087 | | 0.091 | 0.064 | 0.107 |
| | | 4 | | −0.102 | | 0.428 | | |
| 2798 | $\frac{9}{2}$ | 2 | 0.349 | 0.017 | | −0.016 | 0.115 | −0.033 |
| | | 4 | | 0.009 | | −0.077 | | |
| 2816 | $\frac{11}{2}$ | 2 | −0.412 | 0.007 | | −0.045 | −0.279 | −0.007 |
| | | 4 | | −0.004 | | −0.011 | | |
| 2332 | $\frac{3}{2}$ | 2 | 0.097 | 0.005 | | −0.051 | −0.141 | 0.026 |
| | | 4 | | 0.017 | | −0.121 | | |
| 2869 | $\frac{15}{2}$ | 4 | | −0.068 | | 0.374 | | |
| 2959 | $\frac{13}{2}$ | 4 | | −0.107 | | 0.582 | | |
| 3051 | $\frac{7}{2}$ | 0 | 0.200 | 0.071 | 0.078 | | | |
| | | 2 | 0.212 | 0.002 | | 0.029 | −0.061 | 0.015 |
| | | 4 | | 0.020 | | −0.142 | | |
| 3102 | $\frac{3}{2}$ | 2 | −0.443 | −0.019 | | −0.207 | 0.021 | 0.040 |
| | | 4 | | 0.087 | | −0.333 | | |
| 3281 | $\frac{7}{2}$ | 0 | | −0.055 | 0.118 | | | |
| | | 2 | −0.281 | −0.028 | | 0.094 | 0.021 | 0.049 |
| | | 4 | | −0.073 | | 0.483 | | |
| 3289 | $\frac{5}{2}$ | 2 | 0.354 | 0.091 | | −0.110 | −0.177 | −0.013 |
| | | 4 | | 0.081 | | −0.233 | | |
| 3372 | $\frac{1}{2}$ | 4 | | 0.084 | | −0.650 | | |
| 3438 | $\frac{9}{2}$ | 2 | 0.140 | −0.085 | | 0.211 | 0.036 | 0.250 |
| | | 4 | | −0.112 | | 0.499 | | |
| 3663 | $\frac{11}{2}$ | 2 | 0.607 | −0.038 | | 0.092 | −0.314 | 0.118 |
| | | 4 | | −0.009 | | 0.024 | | |
| 3774 | $\frac{13}{2}$ | 4 | | −0.050 | | 0.240 | | |
| 3905 | $\frac{11}{2}$ | 2 | −0.052 | −0.069 | | 0.164 | 0.032 | 0.128 |
| | | 4 | | −0.091 | | 0.608 | | |
| 4214 | $\frac{1}{2}$ | 4 | | 0.016 | | −0.173 | | |
| 4381 | $\frac{15}{2}$ | 4 | | −0.124 | | 0.722 | | |
| 4479 | $\frac{13}{2}$ | 4 | | −0.013 | | 0.109 | | |
| 4697 | $\frac{15}{2}$ | 4 | | −0.013 | | −0.018 | | |
| 4859 | $\frac{1}{2}$ | 4 | | 0.024 | | 0.329 | | |
| 5096 | $\frac{13}{2}$ | 4 | | −0.044 | | 0.115 | | |
| 5703 | $\frac{15}{2}$ | 4 | | 0.065 | | −0.216 | | |

A $(1f_{5/2}, 1f_{5/2})$ configuration was used to calculate $L = 0$, 2, and 4 transfers while $(2p_{1/2}, 3s_{1/2})$ was used for an $L = 1$ transfer and $(1f_{5/2}, 1g_{9/2})$ was used for an $L = 3$ transfer. From the selection rules for a direct, one step $(t,p)$ reaction, the even values of transfered angular momentum would require positive parity for these states whereas the odd values would require negative parity.

The calculated angular distributions, for which the shell-model spectroscopic amplitudes listed in Tables IV and V were used and for which the correspondence between experimental and theoretical levels shown in Fig. 7 was used, are represented by solid curves in Figs. 3 and 5. Each theoretical angular distribution has been independently normalized to the data, and the resulting value of $\epsilon$ for each level has been listed in Table VI. For those levels above 2.5 MeV in $^{52}$Ti, the curves in Fig. 4 are for those DWBA calculations which did not use the shell model two-nucleon transfer spectroscopic amplitudes. The association between the theoretical and experimental levels for states in $^{57}$Mn are shown in Fig. 7. The experimental angular distributions for the $^{57}$Mn states are presented in Fig. 8. The DWBA curves in Fig. 8 were generated using the optical-model parameters from Table I and the two-nucleon-transfer spectroscopic amplitudes given in Ref. 8.

Two questions may be addressed by studying the angular distributions in Figs. 3, 5, and 8: How well does the assumed reaction mechanism describe these angular distributions and how well does the shell model predict the data? A test of the reaction mechanism can be made by studying the transfer between states in two even-even nuclei. The present DWBA calculation assumes a direct, zero-range, one-step transfer of a zero-spin, dineutron pair. With the assumption that the dineutron pair has zero spin and that no spin reorientation occurs, the selection rules allow only a single transferred angular momentum $L$ between even-even nuclei. Since it is the $L$ transfer which determines the shape of the calculated angular distribution and not the various two-nucleon configurations which the two neutrons may occupy in the final nucleus, the single $L$ transfer restriction requires that the angular distribution have a unique shape. A comparison of the data and the calculated angular distribution then indicates whether or not the reaction is proceeding by means of the assumed reaction mechanism.

For the present experiment, the shapes of the DWBA calculated angular distributions are in excellent agreement with the $^{52}$Ti data below 4 MeV which indicates that the primary reaction

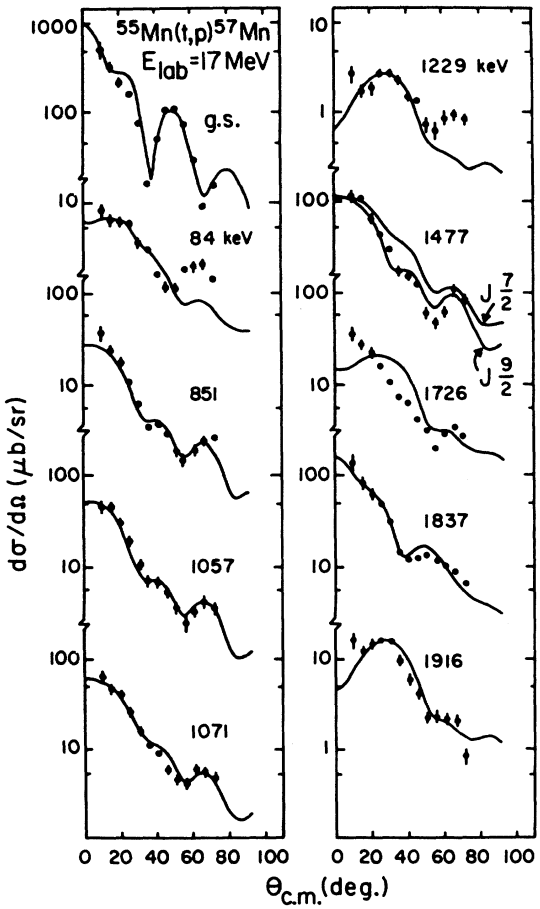


FIG. 8. Experimental $^{57}$Mn angular distributions taken from Ref. 8. The curves are from DWBA calculations which used the shell-model two-nucleon transfer spectroscopic amplitudes listed in Ref. 8.

mechanism is the direct transfer of a zero-spin, dineutron pair. Above 4 MeV, however, the DWBA description of the data becomes poor. An obvious shortcoming of the DWBA is its inability to describe the highly excited $J^\pi = 0^+$ or $1^-$ levels at 4098, 4212, and 4324 keV. These levels are strongly populated and other processes, such as compound nuclear or two step, would not be expected to have this strength at these energies.

The $J = \frac{1}{2}^-$ state at 1057 keV in $^{57}$Mn, which can be populated only by an $L = 2$ transfer, is very well described. The shape of an $L = 4$ angular distribution, as evidenced by the 1229-keV level in $^{57}$Mn, is not as well predicted by the calculation. It should be noted, however, that at angles near 60° where the data are underpredicted by the calculations, the experimental cross section is less than one microbarn. Other processes, such as compound nuclear or two step, could certainly have cross sections of this magnitude. However, the disagreement between the experimental and

theoretical angular distribution shapes may be an indication that the present shell-model configuration space is too restrictive. If the spin of the 1229-keV state is $\frac{11}{2}$, then the allowed angular momentum transfer $L$ could have values of 6 and 8, in addition to 4. However, two-neutron configurations which allow the larger angular momentum transfer have not been included in the present configuration space [e.g., $(1f_{7/2}^{-1}, 1f_{5/2})$]. The higher angular momentum transfer would give rise to an increased back angle cross section. If the level at 1916 keV is also a $J=\frac{11}{2}$ state (as would be supported by the lack of $\beta$ decay feeding to this level), then the shape of the calculated $L=4$ angular distribution is in this case satisfactory.

The shell-model spectroscopic amplitudes for the various two-nucleon configurations in the final nucleus may be tested in two ways. First, for $(t,p)$ reactions on odd-$A$ nuclei, multiple $L$ transfers are allowed to each state in the residual nucleus. It is the shell-model spectroscopic amplitudes which determine the various angular momentum admixtures to each final state and, consequently, which determine the shape of the final-state angular distribution since the $L$ transfer to each state is not unique.

For $^{53}$V, all of the excited states below 2.1 MeV (with the exception of the 1852-keV level) have experimental angular distributions dominated by $L=2$ shapes. The DWBA calculations using the shell-model spectroscopic amplitudes predict predominantly $L=2$ shapes for these angular distributions. On the other hand, where one has substantial $L=0$ and 2 components in the experimental angular distribution for the 1852-keV level, the $L$ admixture is also well reproduced.

A similar situation occurs for levels in the $^{57}$Mn nucleus. Most of the low-lying excited states have predominantly $L=2$ experimental shapes; however, there are those states which have strong $L=0$ and/or 4 admixtures in their experimental angular distributions. With the exception of the 1726-keV state, the shell model correctly predicts the $L$ admixtures for all levels below approximately 2 MeV.

The experimental shape of the 1726-keV level is the only one not reproduced in this analysis. If this level is indeed the $J=\frac{3}{2}$ level, as would be supported by the $\beta$-decay results for this level,[16] then the shell model has failed in predicting this $L$ admixture. This again seems to indicate that valence proton or core excitations of neutrons out of the $1f_{7/2}$ subshell and into the $2p_{3/2}$ subshell are important even at these low excitation energies and that the present configuration space is too limited.

A second test of the shell-model spectroscopic amplitudes is the comparison of the magnitudes of the experimental and theoretical cross sections. Listed in Table VI is the ratio $\epsilon$ of the experimental to theoretical cross section for each level in the three nuclei for which there was a reasonably clear correspondence between the experimental and shell-model state. Although it would appear from this table that the calculated ground-state cross sections overestimate the experimental ground-state strengths by as much as a factor of 2, uncertainties in the absolute experimental cross section, in the Flynn normalization constant $N$, and in the DWBA cross section which arises because of optical-model parameter ambiguities could easily account for a factor of 2. To facilitate a comparison of the relative cross-section predictions, the excited state $\epsilon$'s have been normalized to a ground state $\epsilon$ of one (see $\epsilon_R$ in Table VI).

Although the predictions of the cross sections are not good in all cases, the calculations are able to reproduce important features of the experimental data. In particular, the calculations predict small cross sections for weak experimental levels (for example, the approximately 5 $\mu$b cross sections for the 84- and 1229-keV levels in $^{57}$Mn) and large cross sections for the strongly populated states (the 1000 $\mu$b cross section for the 1050-keV level in $^{52}$Ti as well as the 400 $\mu$b cross section for the 1852-keV $^{53}$V level).

## V. SUMMARY AND CONCLUSIONS

The excitation energies of 19 levels in $^{52}$Ti below 5.1 MeV and 52 levels in $^{53}$V below 4.7 MeV have been measured. Of these, 10 levels in $^{52}$Ti and 13 levels in $^{53}$V had not been reported previously. Spin assignments, or at least spin limitations, could be made to 16 of the levels in $^{52}$Ti from the $(t,p)$ angular distributions. No disagreements were found between any of these assignments and the six spin assignments made in an earlier $^{50}$Ti$(t,p\gamma)^{52}$Ti experiment.[12] In $^{53}$V, no discrepancies were found between the spin assignments suggested in Refs. 10, 14, and 15 and the spin limitations imposed by the $L$ values extracted from the $(t,p)$ angular distributions.

A shell-model calculation in which a $^{48}$Ca core was assumed has been performed for both $^{52}$Ti and $^{53}$V. In an earlier study,[8] a similar shell-model calculation was reported for $^{57}$Mn. The predicted energy-level schemes for these three nuclei are in agreement with the experimental level schemes up to 1.5 MeV. However, it is in this excitation region in $^{57}$Mn that the shell model

TABLE VI. Comparison of experimental and calculated magnitudes of angular distributions for states in $^{52}$Ti, $^{53}$V, and $^{57}$Mn.

| $^{52}$Ti | | | | | $^{53}$V | | | | | $^{57}$Mn | | | | |
|---|---|---|---|---|---|---|---|---|---|---|---|---|---|---|
| $E_x$[a] (keV) | $E_x$(SM)[b] (keV) | $J^\pi$ | $\epsilon$[c] | $\epsilon_R$[d] | $E_x$[a] (keV) | $E_x$(SM)[b] (keV) | $2J^\pi$ | $\epsilon$[c] | $\epsilon_R$[d] | $E_x$[a] (keV) | $E_x$(SM)[b] (keV) | $2J^\pi$ | $\epsilon$[c] | $\epsilon_R$[d] |
| 0 | 0 | $0^+$ | 0.50 | 1.00 | 0 | 0 | $7^-$ | 0.53 | 1.00 | 0 | 0 | $5^-$ | 0.72 | 1.00 |
| 1050 | 1028 | $2^+$ | 0.29 | 0.58 | 127 | 26 | $5^-$ | 0.20 | 0.38 | 84 | 110 | $7^-$ | 2.04 | 2.83 |
| 2262 | 1879 | $2^+$ | 0.45 | 0.90 | 226 | 192 | $3^-$ | 0.22 | 0.42 | 851 | 850 | $3^-$ | 0.21 | 0.29 |
| 2316 | 2346 | $(4^+)$ | 0.19 | 0.38 | 1093 | 1196 | $11^-$ | 0.85 | 1.60 | 1057 | 1200 | $1^-$ | 0.29 | 0.41 |
| 2429 | 1879 | $2^+$ | 0.20 | 0.40 | 1269 | 1213 | $9^-$ | 0.42 | 0.79 | 1071 | 1230 | $9^-$ | 0.40 | 0.56 |
| | | | | | 1551 | 1763 | $5^-$ | 0.31 | 0.58 | 1229 | 1310 | $11^-$ | 1.56 | 2.20 |
| | | | | | 1652 | 2197 | $9^-$ | 0.13 | 0.25 | 1477 | 1420 | $9^-$ | 0.36 | 0.50 |
| | | | | | 1852 | 2131 | $7^-$ | 0.28 | 0.52 | | 1540 | $7^-$ | 0.91 | 1.26 |
| | | | | | 1901 | 2097 | $3^-$ | 0.49 | 0.92 | 1726 | 1720 | $3^-$ | 2.32 | 3.31 |
| | | | | | 2079 | 2097 | $3^-$ | 0.09 | 0.17 | 1837 | 1820 | $5^-$ | 0.33 | 0.46 |
| | | | | | | | | | | 1916 | 1970 | $11^-$ | 0.44 | 0.60 |

[a] Experimental excitation energies.
[b] Shell-model predicted excitation energies.
[c] $\epsilon$ from Eq. (1).
[d] $\epsilon$ of states when the ground state $\epsilon$ is normalized to 1.

prediction breaks down. Three levels with $J^\pi \leq \frac{5}{2}$ have been observed at excitation energies of 1375, 1493, and 1536 keV while only one level has been predicted theoretically (see Fig. 7) in this region with $J^\pi \leq \frac{5}{2}$. Further, there does not appear to be a likely shell-model level which could account for these "intruder" experimental levels for at least 500 keV. A similar breakdown in the shell-model calculations appears to occur in both $^{52}$Ti and $^{53}$V. In $^{53}$V the sequence of predicted levels is incorrect between 1.5 and 2.1 MeV and again there seems to be an additional experimental level with spin of either $\frac{3}{2}$ or $\frac{5}{2}$ in this energy region. Another serious deficiency in the shell-model calculation is evident when the calculated and experimental $^{52}$Ti spectra are compared. The shell model has accounted for only one of the two $2^+$ levels around 2.3 MeV in energy. In addition, if the lower $2^+$ level does indeed correspond to the predicted $2^+$ level, then the energy of this calculated state is incorrect by nearly 400 keV.

Shell-model calculations in this mass region have not, in general, been able to account for a number of low-lying experimental levels. A common feature of these calculations is that nucleon excitation out of the $1f_{7/2}$ subshell was not allowed. Recent shell-model calculations by Johnstone and Benson,[6,7] which include not only the lowest $(p_{3/2}f_{5/2}p_{1/2})^n pf_{7/2}^n h$ configuration relative to the closed-shell state of $^{56}$Ni but also include configurations in which at least one of the $f_{7/2}$ nucleons has been promoted to a higher subshell have been more successful. The promotion of only one additional nucleon in many cases accounts for all of the "intruder" experimental levels which have occurred at excitation energies as low as 750 keV.

According to the Johnstone and Benson shell-model calculations, these levels which arise from the $f_{7/2}$ nucleon excitations have rather pure configurational structure and, consequently, are not strongly mixed with the remaining levels. The present DWBA calculations gave fair agreement for the shapes and relative magnitudes of the $(t,p)$ angular distributions for most of the low-lying $^{52}$Ti, $^{53}$V, and $^{57}$Mn levels when the current shell-model spectroscopic amplitudes were employed. Hence, our results are consistent with the idea of weak mixing between the two types of states.

We acknowledge financial support from the National Science Foundation and the U. S. Department of Energy (Contract No. W-7405-eng-26 with the Union Carbide Corporation).

*Present address: Physics Department, Tennessee Technological University, Cookeville, Tennessee 38501.
†Present address: Bell Laboratories, Holmdel, New Jersey 07733.

[1] J. B. McGrory, Phys. Rev. 160, 915 (1967).
[2] J. Vervier, Nucl. Phys. 78, 497 (1966).
[3] H. Horie and K. Ogawa, Nucl. Phys. A216, 407 (1973).
[4] J. B. McGrory, B. H. Wildenthal, and E. C. Halbert, Phys. Rev. C 2, 186 (1970).

[5]K. Lips and M. T. McEllistrom Phys. Rev. C 1, 1009 (1978).
[6]I. P. Johnstone, Phys. Rev. C 17, 1428 (1978).
[7]I. P. Johnstone and H. G. Benson, Phys. Rev. C 17, 311 (1978); J. Phys. G 3, L69 (1977).
[8]J. F. Mateja, C. P. Browne, C. E. Moss, and J. B. McGrory, Phys. Rev. C 15, 1708 (1977).
[9]N. B. Gove and A. H. Wapstra, Nucl. Data Tables 11, 127 (1972).
[10]L. A. Parks, C. N. Davids, and R. C. Pardo, Phys. Rev. C 15, 730 (1977).
[11]S. Hinds and R. Middleton, Nucl. Phys. A92, 422 (1967).
[12]J. G. Pronko, T. T. Bardin, J. A. Becker, T. R. Fisher, R. E. McDonald, and A. R. Poletti, Phys. Rev. C 9, 1430 (1974).
[13]J. R. Beene, Nucl. Data Sheets 25, 235 (1978).
[14]S. Hinds, H. Marchant, and R. Middleton, Phys. Lett. 24B, 34 (1967).
[15]J. G. Pronko, T. T. Bardin, and J. A. Becker, Phys. Rev. C 13, 608 (1976).
[16]C. N. Davids, D. F. Geesaman, S. L. Tabor, M. J. Murphy, E. B. Norman, and R. C. Pardo, Phys. Rev. C 17, 1815 (1978).
[17]P. D. Kunz (private communication).
[18]R. E. Casten, E. R. Flynn, Ole Hansen, and T. J. Mulligan, Phys. Rev. C 4, 130 (1971); E. R. Flynn, D. D. Armstrong, J. G. Beery, and A. G. Blair, Phys. Rev. 182, 1113 (1969).
[19]F. G. Perey, Phys. Rev. 131, 745 (1963).
[20]E. R. Flynn, J. D. Sherman, N. Stein, D. K. Olsen, and P. J. Riley, Phys. Rev. C 13, 568 (1976).